Table S1. SAXS data collection, analysis, and modeling fitting.

(a) Sample details

	CD97	CD55	chimeric complex
Organism		Homo sapiens	
Source (Catalogue No. or reference)		HEK293S GnTI- expressed	
UniProt sequence ID (residues in construct)	P48960(21-165)	P08174(35-285)	CD97-24a-CD55
Extinction coefficient ε (A280, $M^{-1\ cm-1}$)	22095	39390	68475
Partial specific volume ($cm^3\ g^{-1}$)	0.715	0.718	0.723
Mean solute and solvent scattering length densities	12.361/9.489	12.365/9.489	12.528/9.489
mean scattering contrast Δρ (cm^{-2})	2.872	2.876	3.039
Molecular mass M from chemical composition (KDa)	16.6	28.6	46.8
Concentration (range/values) measured and method	0.5-2	0.5-2	0.5-2
Solvent composition and source		20 mM Tris 7.5,200 mM NaCl and 2 mM $CaCl_2$	

(b) SAS data collection parameters

Source, instrument and description or reference	Ref. J. Appl. Cryst. (2016) 49, p1428-1432
Wavelength (Å)	0.9184
Beam geometry (size, sample-to-detector distance)	340μm x 60μm (H x V), 2.415m
q-measurement range (Å-1 or nm-1)	0.008-0.47
Basis for normalization to constant counts	Take silver behenate as standard to set the mask, then normalize 2D images
Method for monitoring radiation damage, X-ray dose dose where relevant	SAXS data were collected as continuous serial exposures and scattering profiles for the passes were compared to monitor the radiation damage
Exposure time, number of exposures	1 s per frame, total 20 frames
Sample temperature (ºC)	10

(c) Software employed for SAS data reduction, analysis and interpretation

SAS data reduction	*ln I(q)* versus *q* using *OriginPro 8* (http://www.OriginLab.com), solvent substraction using *PRIMUS* (*ATSAS 2.8.0;* Franke *et al*., 2017)
Extinction coefficient estimate	http://protcalc.sourceforge.net/
Calculation of Δρ and ΔV values from chemical compo	MULChe ref.Whitten et al., 2008
Basic analyses: Guinier, P(r), Vp	*PRIMUS* (*ATSAS 2.8.0*; Franke et al., 2017)
volume (e.g. Porod volume VP or volume of correlatio	PRIMUS (ATSAS 2.8.0; Franke et al., 2017)
Shape/bead modelling	*GASBOR*(Svergun *et al.*, 2001) and *DAMAVER* (Volkov *et al*., 2003)
Molecular graphics	*PyMOL*

(d) Structural parameters

	CD97	CD55	chimeric complex
Guinier Analysis			
I(0) (a.u)	11.82±0.32	16.27±0.23	15.11±0.21
Rg (Å)	28.27 ± 0.34	41.60 ± 0.56	33.56 ± 0.39
q-range ($Å^{-1}$)	0.0255-0.0456	0.0187-0.03121	0.0259-0.0384
Quality-of-fit parameter (with definition)	0.71	0.79	0.88
P(r) analysis			
I(0) (a.u)	12.47	16.34	17.38
Rg (Å)	31.07	43.75	41.43
dmax (Å)	99.5	142.5	142.5
q-range ($Å^{-1}$)	0.0255-0.0456	0.0187-0.03121	0.0259-0.0384
Quality-of-fit parameter (with definition)	0.753	0.737	0.792
Volume (e.g. VP and/or Vc)	39190	36290	72750

(e) Shape modelling results (a complete panel for each method)

	CD97	CD55	chimeric complex
q-range for fitting ($Å^{-1}$)	0.0080-0.4068	0.0080-0.4068	0.0080-0.4068
Symmetry/anisotropy assumptions	P1	P1	P1
χ^2 value/range	3.09	5.27	2.23
Model volume and/or *M* estimate	41742	41878	50600
Model precision/resolution	2.394	1.982	1.982

(f) Atomistic modelling

	CD97	CD55	chimeric complex
Method	PyMol	PyMol	PyMol
q-range for fitting	0.0138-0.4049	0.0138-0.4049	0.0134-0.4041
Symmetry assumptions	P1	P1	P1
Any measures of model precision	NSD	NSD	NSD
NSD value, any other quality-of-fit parameters	2.99	2.83	2.74

(g) Data and model deposition IDs

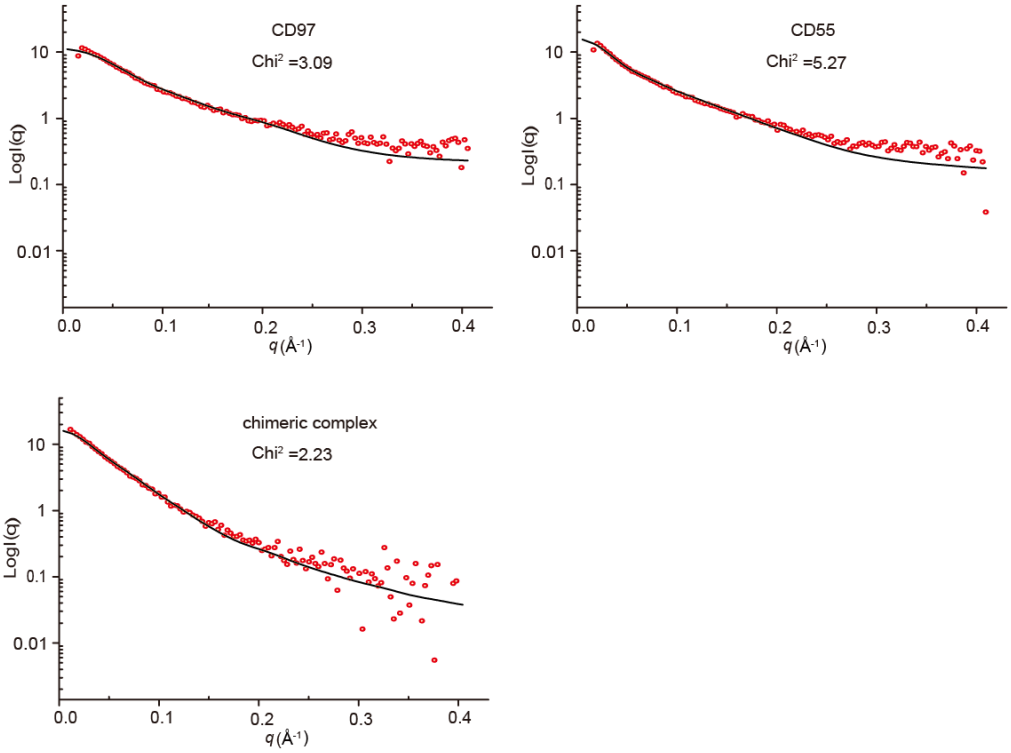

Fig. S1. Raw SAXS data (red points) and fits (black lines) of the CD97–CD55 chimeric complex and individual proteins.

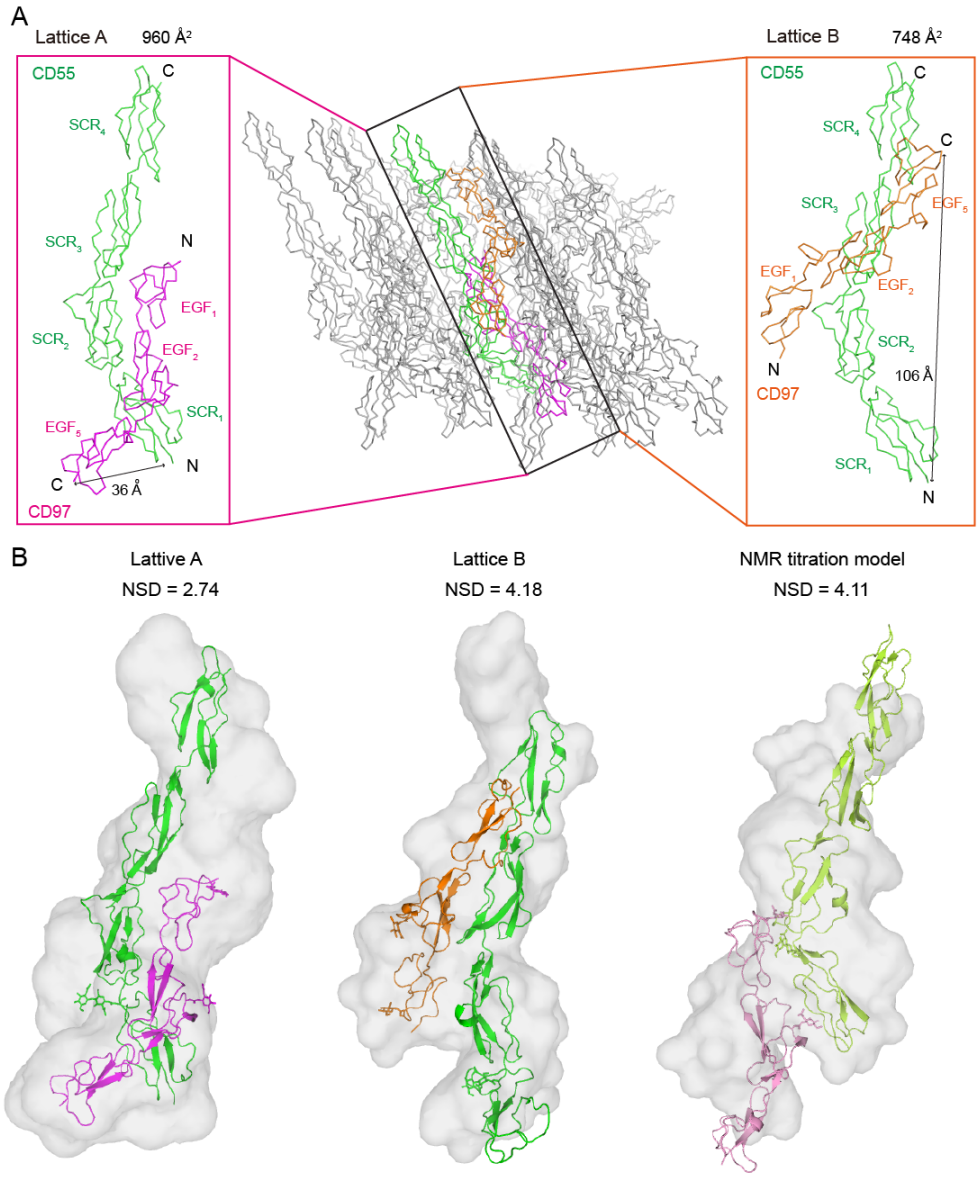

Fig. S2. The packing interfaces and alignments with SAXS envelop of the CD97–CD55 complex. (A) Two major lattices are shown in the pink and orange frames, respectively. Lattice A indicates anti-parallel interaction involving the N-terminal domains of each individual protein; whereas the Lattice B shows a parallel interaction composing each C-terminal domains, which is contradictory with a canonical trans-type ligand-receptor interaction and several recent studies. (B) The two lattices and previous NMR titration model are superimposed with the calculated SAXS envelop of the complex. Lattices A and B are colored according to panel A, while the CD97 and CD55 in the NMR titration model are colored light red and light green, respectively. Smaller NSD (normalized structural difference) indicates better alignment.

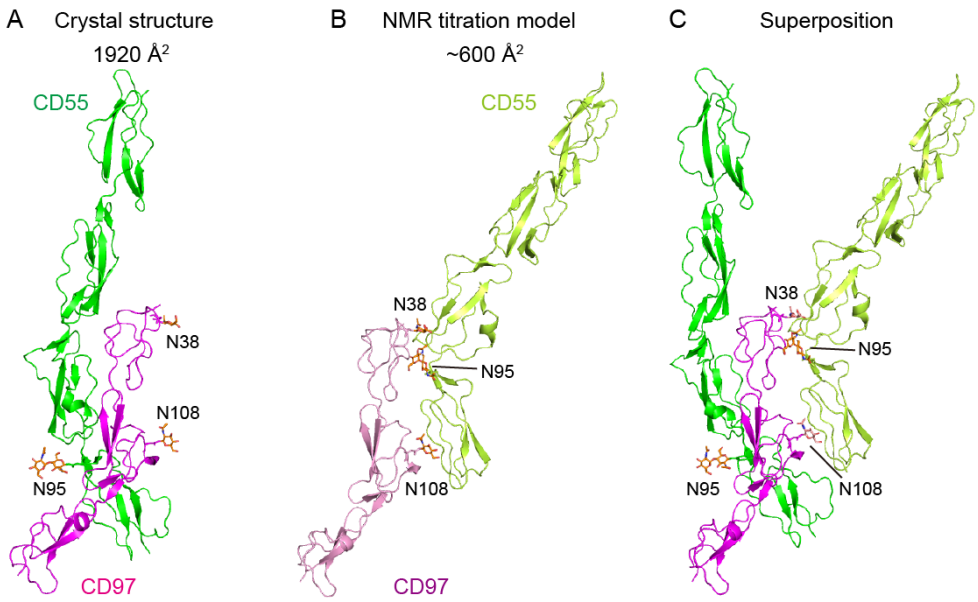

Fig. S3. Comparison of the crystal structure with previous NMR titration model.

The crystal structure (A) and NMR titration model (B) are shown with same orientation on CD97. The NMR titration model is prepared based on figures from previous paper[23]. N-glycosylation sites are shown as sticks and marked. C. The two models are superimposed on CD97.

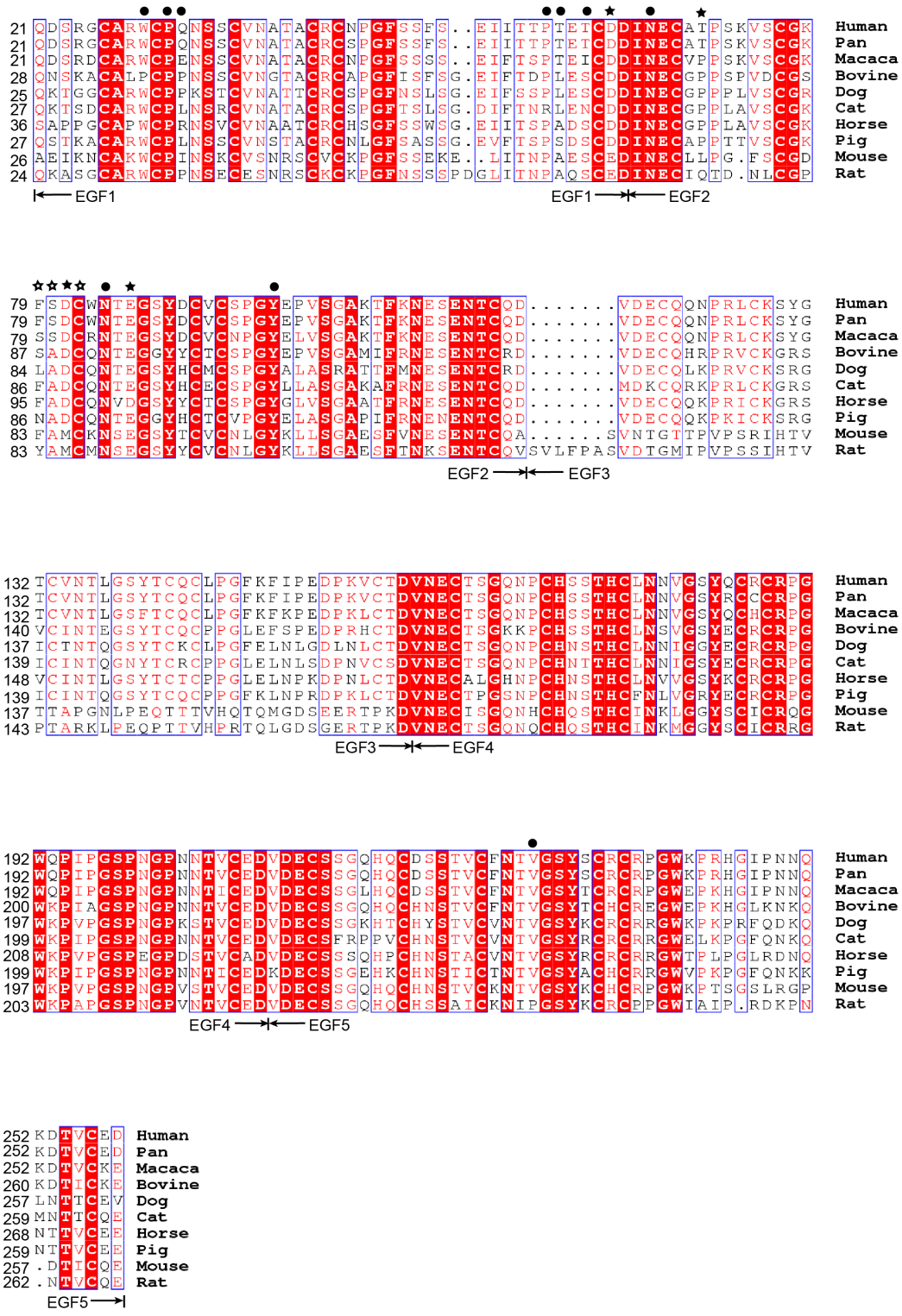

Fig. S4. Sequence alignment of CD97 EGF domains.All five EGF domains of different species were aligned with each EGF domain boundary marked. Each rodent (rat/mouse) CD97 contains a sequence of ~45-residues in the middle and their EGF3 and EGF4 align well with others' 4th and 5th EGF domains. CD55-interacting residues are marked with solid dots, while hydrogen-bonded residues are marked with solid (side chain) and empty (main chain) asterisks.

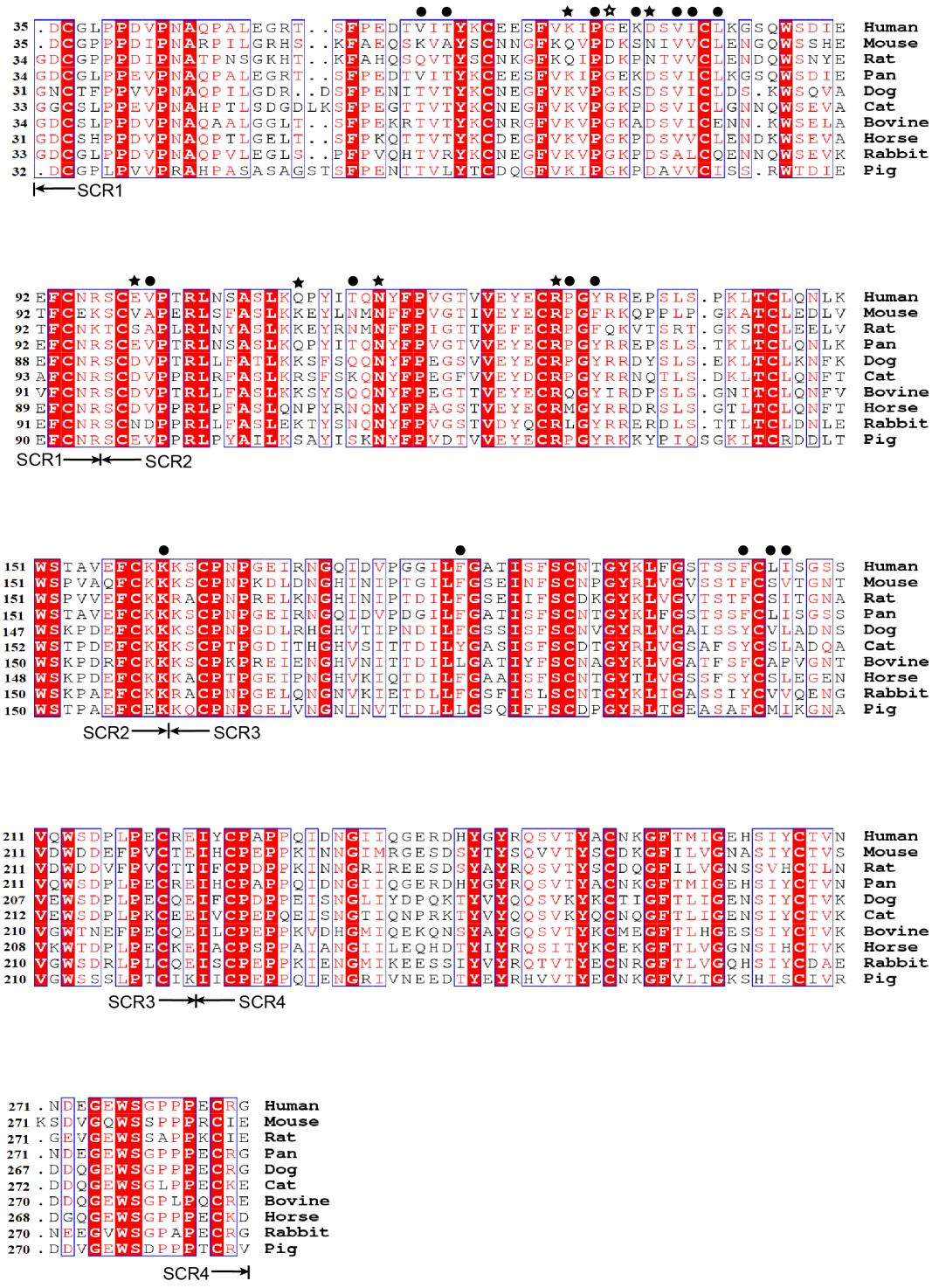

Fig. S5. Sequence alignment of CD55 SCR domains.

Domain boundaries were marked and CD97-interacting residues were marked as supplementary figure 4.

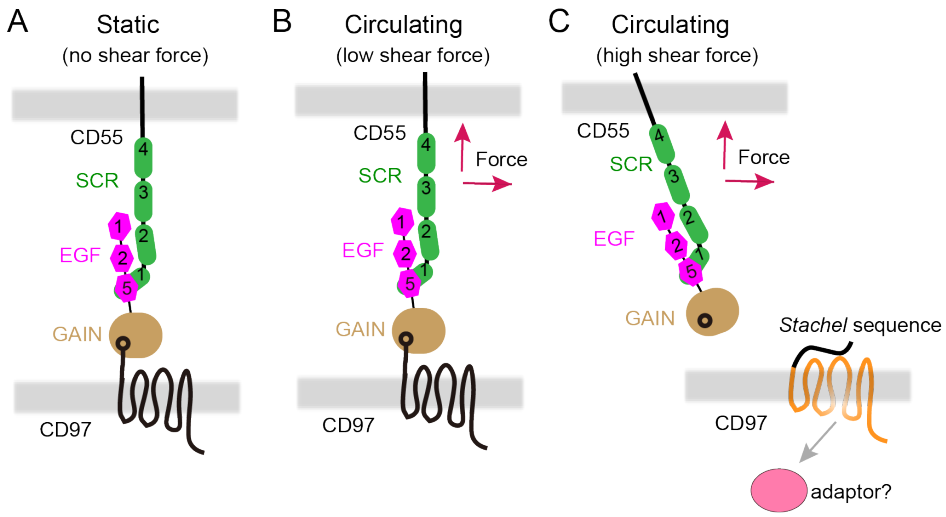

Fig. S6. The CD97–CD55 interaction and signaling.

In static (A) or low shear force (B) tissues, contacts between receptor CD97 and one of its ligands CD55 can withstand a significant range of shear force thus facilitate cell adhesion. The binding modality of CD97 and CD55 suggests a shearing stretch geometry, and indicates transmission of force from the binding interface to the following GAIN and 7TM domains. When the shear force is large enough (C), it can induce conformational change of the GAIN domain and release of the *Stachel* sequence. For example, in inflammation site, certain population of the extracellular region was stretched away by CD55 and dissociated from the cell membrane, thus the leukocytes will not be over clustered. The exposed *Stachel* sequence may reorient and dock to the 7TM domain and trigger downstream signaling, although a downstream adaptor has yet to be identified for CD97.